Soft Matter

Cite this: *Soft Matter*, 2012, **8**, 6684

www.rsc.org/softmatter

COMMUNICATION

Interfacial polymer phase segregation and self-assembly of square colloidal crystals†

Matthew M. Shindel,[a] Szu-Wen Wang[b] and Ali Mohraz*[b]

Received 11th August 2011, Accepted 8th May 2012
DOI: 10.1039/c2sm25808k

Polystyrene colloids exhibit unique bimodal dynamics at the air–water interface in the presence of PEG polymers. We attribute this to agglomeration of the polymer into polymer-rich and polymer-sparse domains at the interface. Colloids adsorbed to polymer-depleted regions retain mobility and self-assemble into two-dimensional crystals with square symmetry, which is ascribed to an undulated contact line on the particles and the droplet's negative Gaussian curvature. To our knowledge, this is the first example of thermodynamically favoured two-dimensional square crystals formed by means of interfacial colloid assembly.

Under near-neutral wetting conditions, colloidal particles can exhibit interfacial activity similar to that of molecular surfactants.[1] This propensity to adhere to a fluid–fluid interface has been exploited to impart mechanical and kinetic stability to microscale bubbles,[2] emulsions,[3] foams,[4] and bicontinuous emulsion gels.[5] Consequently, interfacially active colloids are valued in widespread technological applications such as consumer health and food products, controlled packaging, transport and release of molecular therapeutics or other chemical/biochemical agents,[6,7] and the fabrication of functional, macroporous materials.[8] Furthermore, fluid–fluid interfaces can serve as venues for the self-assembly of two-dimensional (2-D) colloidal crystals whose geometrically repetitious microstructure can be exploited in photonic and lithographic applications.[9,10] However, control over crystal lattice geometry is currently limited. Both thermal[1,11] and convective[12] 2-D crystallization processes in monodispersed, spherical particle populations tend to favor the formation of hexagonal arrays unless an external (physical or energetic) template[13–15] or electric field[16] is applied to the system. In the latter case, non-hexagonal symmetries have only been observed with Janus particles, which can experience anisotropic interparticle interactions in an external field.

In this communication, we report on unique interfacial phase behavior and colloidal crystallization processes observed in dilute, aqueous mixtures of aminated polystyrene colloids (D = 1 μm; Molecular Probes) and methoxy-poly(ethylene glycol) molecules possessing a carboxyl functional group at one end (M_w = 1140 Da; Creative PEGworks). When droplets of this mixture are placed in contact with air, both colloids and polymer molecules diffuse from the bulk and adhere to the air–water boundary. Interestingly, once sequestered at the fluid–fluid interface, some isolated particles are found to be Brownian, while others are dynamically arrested. The bimodal distribution of particle dynamics suggests the coexistence of interfacial domains with different microrheological characteristics, which we attribute to spontaneous phase segregation of the polymer at the interface. Furthermore, the mobile particle population subsequently self-assembles into 2-D crystals (co-planar with the air–water interface) with square lattice geometry. Thus, the work detailed here exposes the following distinctive interfacial phenomena in this system: (1) spontaneous partitioning of mono-functionalized PEG molecules at the air–water interface and the capture and immobilization of colloidal particles in PEG-rich domains, and (2) interfacial self-assembly of 2-D square colloidal crystals in the absence of either an externally applied field or a template. Our findings may unveil new avenues for engineering patterned surfaces, lithographic templates, photonic materials, and particle separation technologies.

In our experiments, fluorescent aminated polystyrene particles were washed by a minimum of five rounds of centrifugation, decantation, and re-suspension in water, and thoroughly mixed with dissolved methoxy-poly(ethylene glycol)–acetic acid (mPEG–AA) in Milli-Q water. The final particle and polymer concentrations were 0.2% w/v and 0.03% w/v, respectively. In a given experiment, a 5 μl droplet of the colloid–polymer suspension was supported by a glass coverslip(s) in either a hanging-drop (hd) or capillary-bridge (cb) configuration (Fig. 1). The liquid was maintained in an enclosed, humidified environment to minimize evaporation and prevent mechanical perturbations arising from ambient air currents.

Particles were imaged with either epifluorescence (Olympus BX51, connected to an ORCA-285 CCD camera, Hamamatsu), or fluorescence confocal microscopy (Axio Observer A1, Zeiss; equipped with a Vt-eye scanner, Visitech International). The boundary demarcating particle-free and particle-occupied regions in the imaging volume was considered to be the air–water interface. Particle centres of mass were identified in confocal images using standard centroiding algorithms[17] written in Interactive Data Language (IDL)

[a]*Department of Chemical Engineering and Center for Molecular and Engineering Thermodynamics, University of Delaware, Newark, Delaware 19716, USA*
[b]*Department of Chemical Engineering and Materials Science, University of California, Irvine, California 92697, USA. E-mail: mohraz@uci.edu*

† Electronic supplementary information (ESI) available: Microscopy videos showing bimodal particle dynamics and colloidal crystallization at the interface, images showing square colloidal crystals in the hd, and calculation of the capillary interparticle potential at a curved interface. See DOI: 10.1039/c2sm25808k

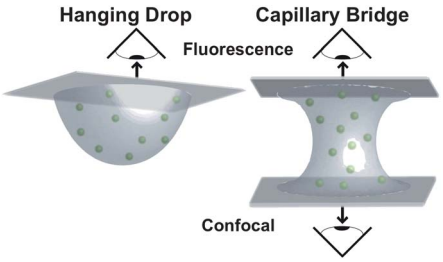

Fig. 1 Illustration depicting the 'hanging drop' (left) and 'capillary bridge' (right) experimental designs.

software, and 3-D representations of confocal image volumes were rendered using Mayavi2 software package.[18,19]

After forming the hd or cb, particles successively migrate to and remain at the air–water interface. Two different types of 2-D assemblies evolve on the droplet surface as particles transition from the bulk: disordered arrangements including individual particles and small aggregates, and colloidal crystals (Fig. 2a). In addition to being structurally distinct, the dynamic signatures of the constituent particles within these architectures also differ significantly (ESI, Video 1†). Multiple particle tracking was used to assess the motion of colloids in both the disordered and crystalline arrangements.[17] While particles incorporated into crystalline domains retain some degree of mobility, the flat mean-square displacement (msd) profile extracted from the disordered regions is indicative of arrested dynamics (Fig. 2b). The particle msd obtained in these areas is on the order of the noise level for our imaging system ($\boldsymbol{O}(10^{-3}$ μm)) and therefore reflects redefinition of particle centeroid locations by the tracking algorithm rather than actual particle motion.[20] The bimodal divergence in interfacial particle dynamics is repeatedly observed in both the hd and the cb configurations.

On a larger scale, epifluorescence images show the gradual formation of a tenuous 2-D particle-embedded network at the air–water interface (Fig. 3a). However, the arrested dynamics of particles in the disordered domains is not a collective by-product of assembly, *i.e.* particle mobility is not progressively reduced due to the formation of a percolating particle network. At early time points, individual particles were frequently observed to abruptly lose their Brownian motion and become immobilized in seemingly bare regions of the fluid–fluid boundary. After arrest, if such particles did move a measurable distance, it was in a sluggish and directed manner, typically coherent with gravity. Such motion was often perfectly

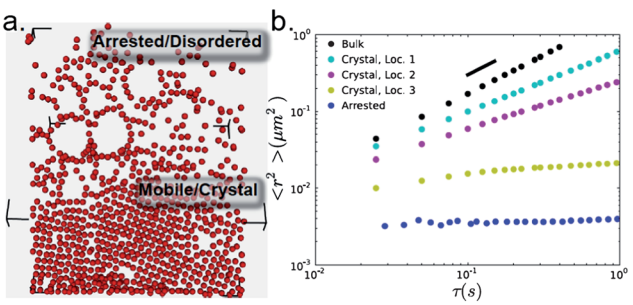

Fig. 2 (a) Interfacial particles rendered from a confocal image volume. (b) Particle msd data acquired from the droplet bulk and the air–water interface. Locations 1, 2 and 3 are shown in Fig. 4.

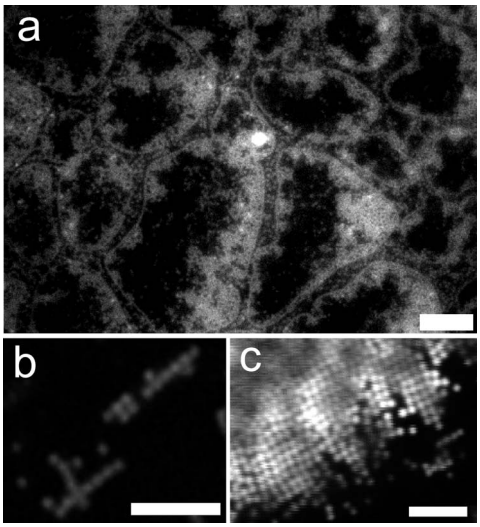

Fig. 3 (a) Epifluorescence image showing a particle-embedded network at the interface. Particles in the islands are mobile. Scale bar = 20 μm. (b) Epifluorescence image of particle chains early in the crystallization process. Scale bar = 10 μm. (c) Confocal image of a square crystal domain. Scale bar = 5 μm.

correlated with other particles residing tens to hundreds of microns away, indicating the formation of polymer 'rafts' on the liquid surface.

Rheological studies have demonstrated that at sufficiently high polymer concentrations, aqueous PEG solutions transition from a Newtonian liquid to a viscoelastic fluid or gel, causing the motion of tracer particles embedded in the fluid to stagnate.[21] PEG has also been shown to possess interfacial activity in aqueous environments.[22,23] It is reasonable to assume that regions of the interface will gain viscoelasticity if the local polymer concentration is sufficiently high. Here, the dynamics of particles trapped at the interface can be used as a proxy for the microrheological environment,[24] which itself depends on the local polymer concentration. Therefore, the coexistence of mobile and immobile particle fractions likely reflects the presence of spatial variations in the concentration of polymer at the interface. Particle mobility is retained in areas where polymer concentration is relatively low, while the immobile particles reside in polymer-rich regions. Particles in the bulk exhibit purely diffusive dynamics (logarithmic slope = 1; Fig. 2b), indicating that the PEG molecules do not self-associate within the droplet interior. Also, the colloid–polymer solution is well-mixed prior to use, allowing for a spatially homogeneous flux of polymer to the interface. Therefore, the heterogeneous PEG distribution must stem from polymer agglomeration or phase segregation occurring exclusively at the air–water interface.

The carboxylated polymer was critical to interfacial assembly. Neither disordered nor crystalline structures were observed in suspensions devoid of mPEG–AA. Thus, the presence of this relatively simple PEG derivative gives rise to disparate interfacial environments, dramatically impacting the particle dynamics and possibly also the interparticle interactions. Furthermore, neither dynamic arrest nor crystallization occurred when mPEG–AA was replaced with a PEG derivative lacking an acidic end-group ($mPEG_{24}$–maleimide, or PEG with M_w = 1500, 8 × 10^3, or 5 × 10^6 Da). The relatively quiescent response to PEG polymers lacking an acidic

functionality suggests that the unique interfacial behaviour of mPEG–AA is linked to intermolecular interactions mediated by the polymer's carboxyl terminus.

In light of the above arguments, the tenuous network (Fig. 3a) presumably results from colloidal particles decorating the segregated polymer domains and is comprised of a polymer-rich backbone, as determined by the arrested particle dynamics in these regions, and discrete polymer-sparse islands. Tighter particle packing is achieved at the polymer phase boundaries, which become clearly demarcated once a significant number of particles have migrated to the interface. The irregular, tenuous geometry of the polymer-rich domains is noteworthy, and suggests that the formation of a percolating, elastic particle network may kinetically hinder the polymer partitioning process.

After translocating from the bulk to the interface, particles that retain their Brownian mobility exhibit a weak attraction towards each other and begin to reversibly assemble into ordered structures regardless of their local interfacial concentration (ESI, Video 2†). This attraction is specific to particles residing at the interface; neither aggregation nor ordering occurs in the bulk liquid. Thus, the interparticle attraction is attributable to capillary interactions incited by the particles locally deforming the air–water interface.[25] This claim is further bolstered by the fact that crystallization (as well as the arrested particle phase) was inhibited when a surfactant (Tween 20) was added to the mixture. Gravity cannot account for the capillarity in this system due to the small particle size (Bo $\ll$ 1).

The conclusion that crystallization is spurred by capillary attraction is relatively intuitive and straightforward given the aforementioned empirical observations. However, very particular requirements must be met for crystal assembly to occur. The mobile particle fraction did not crystallize at planar interfaces, nor did crystallization occur in the absence of mPEG–AA. Thus, two important caveats (explained in greater detail below) are related to the self-assembly process described here: (1) the interface must possess a sufficient degree of curvature (either locally or globally), and (2) interfacial activity, and possibly a rough contact line, must be imparted to the particles by polymer adsorption. Despite residing on dramatically different length scales, the capillary interaction driving crystallization is apparently derived from the conflation of these two effects.

Comparing experiments conducted with the two different droplet geometries provides insight into the role of interfacial curvature in crystal self-assembly. In the hd, crystals were typically found in and/or near irregularities (kinks, fingers, *etc.*) in the three-phase contact line formed where the droplet, glass support and air meet (ESI†). This was also true in the cb; however, crystalline domains were also able to spontaneously arise on smooth regions of the interface far from the contact line. These results suggest that the interface must not only be curved to induce self-assembly, but it must also be endowed with a negative Gaussian curvature.

The initial stages of crystallization typically yield linear particle chains (Fig. 3b; ESI, Video 3†), suggesting that the attractive interparticle interactions are anisotropic. Remarkably, chain orientation is distributed in a binary and orthogonal manner – each chain is aligned parallel to one of the principle axes of curvature for the interface. Further, while chains and small crystallites are able to translate along the liquid surface, they do not rotate, indicating a preferential orientation within the plane of the interface (ESI, Videos 2 and 3†), similar to the behaviour of rod particles on nonplanar surfaces.[26,27] As the process continues, particles self-assemble into crystalline domains with local four-fold-symmetry (Fig. 3c). Crystal growth progresses through both the addition of free particles to existing domains and the coalescence of crystallites and chains (ESI, Videos 2 and 3†). The observed crystal growth in regions of low interfacial particle concentration confirms that ordering is driven by attractive interparticle interactions as opposed to 'crowding'. In addition, the reversible nature of the assembly process shows that square ordering is the equilibrium configuration for this system.

The crystals' square geometry is likely a consequence of an inherent symmetry in the capillary interaction. At an interface possessing a negative Gaussian curvature (such as the cb), the presence of a spherical particle generates quadrupolar deformations aligned with the principle axes of curvature as a consequence of satisfying Young's equation along the particle boundary.[28] On such bifurcated surfaces, the resulting capillary pair-potential is minimized at $\varphi = 0$ and $\pi/2$, where φ is the angle of orientation between the particle pair and the principle curvature axes. Square ordering is therefore plausible under such conditions. However, for 1 μm particles adhered to the capillary bridge interface, the curvature-induced quadrupolar interaction is one to several orders of magnitude below the particles' thermal energy even at small separations (ESI†). Therefore the capillary interaction that drives crystallization cannot be solely attributed to droplet curvature.

The acidic moiety of mPEG–AA can interact with solvent-exposed amines on the surface of the colloids through electrostatics, hydrogen-bonding and/or salt-bridging. We propose that the carboxyl functionality drives adsorption of mPEG–AA molecules onto the colloids, thereby generating 'patchy' particle surfaces that contain local gradients in wettability. Nanometer-scale deviations of the meniscus from the ideal, 'straight-line' conformation can lead to an attractive capillary potential that exceeds the particle thermal energy by several orders of magnitude.[29,30] Deformations of a fluid interface stemming from an irregular contact line are well described by a multipole expansion with a leading quadrupole term, which would favour the formation of a square lattice.[28–31] Direct measurements of the capillary force between metallo-dielectric Janus particles with undulated contact lines have shown the quadrupole moment to be dominant in the far-field at a planar oil–water interface.[32] Yet, the ensuing particle ensembles were fractal-like (indicative of diffusion-limited aggregation), a result potentially attributable to the near-field contribution of higher-order moments in the capillary potential. However, the high polarizability of metals gives rise to a potent (and isotropic) van der Waals force, which could drastically alter the net pair-potential in the near-field, consequently influencing the resulting particle microstructure. In contrast, the reversible nature of the crystallization process in our system (ESI, Videos 2 and 3†) implies that the driving capillary force resides on a kT-scale. Thus, kinetic impediments to ordering are alleviated. Furthermore, as discussed above, the droplet's shape may accentuate the quadrupole moment generated by the undulated contact lines causing it to dominate the interparticle potential in the near-field, and promote the assembly of square crystals.

The ionic double-layer repulsion, which stabilizes particles in the bulk, can serve as an additional bias towards square ordering. Denser packing would increase the degree of electrostatic shell overlap between particles in a cluster. As shown in Fig. 4, while the interfacial lattice predominantly displays square ordering, regions of hexagonal packing are observed near the base of the cb. This symmetry is solely observed near the bottom of the cb; crystals formed at the top of the

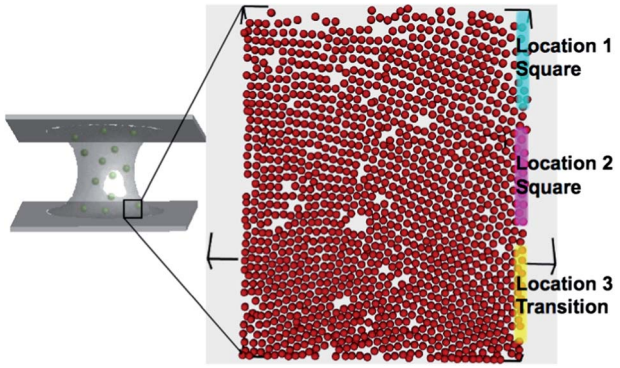

Fig. 4 Crystalline particle lattice rendered from a confocal image volume. Approximate locations at which particle dynamic data (Fig. 2b) was obtained are marked.

image volume are devoid of hexagonal order. In addition, the msd data obtained at different vertical locations within the crystal (Fig. 2b) show a gradual suppression of particle mobility as the vertical height is reduced, from nearly diffusive behaviour in the top layers to a plateaued msd showing particle 'caging' near the bottom. Therefore, the structural transition from the equilibrium square configuration to hexagonal crystals is concomitant with a suppression of particle dynamics, and is probably induced by gravitational compression.

We have stipulated that mPEG–AA is required for the formation of both crystalline and disordered particle structures. These assembly processes are distinct phenomena and the two types of structures arise simultaneously and independently of each other. Yet, the collective interfacial behaviour of the polymer molecules and particles strongly depends on polymer end-group chemistry and molecular weight. Substituting mPEG–AA (1 kDa) with a higher molecular weight analogue (mPEG–AA 2 kDa, 0.03% w/v) resulted in the formation of square crystals but did not generate any arrested particle domains. This is probably due to an increased solubility and reduced interfacial activity of the higher-molecular weight polymer. Experiments in which solution pH was varied by the addition of strong acid or base were also conducted to gain further insight into the role of electrostatic interactions. Because the carboxyl moiety of mPEG–AA is a weak organic acid, the relative fractions of protonated and deprotonated polymer molecules can be tuned by adjusting pH. The interfacial behaviour of both the particles and the polymer changed with pH, but colloidal stability in the bulk was unaffected. It is reasonable to expect that both forms of the polymer molecule are present in significant relative quantities at the mixture's natural pH (4.0–4.5), since the pK_a of acetic acid is ~4.7. Altering the acid–base equilibrium to favour the protonation of polymer molecules, through the addition of concentrated HCl (final concentration of 1 or 10 mM), promotes particle arrest and subsequent formation of disordered structures throughout the interface. In this case mobile particles or colloidal crystals were not observed. Favouring the deprotonated form of polymer, *via* addition of NaOH (to a final concentration of 1 or 10 mM), stymies interfacial assembly entirely; neither crystalline nor arrested particle domains are generated. These results suggest that the elastic, polymer-rich phase is formed through intermolecular hydrogen-bonding, largely constituted by the protonated form of the polymer and achieves more expansive interfacial coverage at low pH. Inhibition of crystallization at high pH indirectly supports our model that polymer adsorption on the particles is an indirect requirement for interparticle capillary attraction, and also indicates that electrostatics is probably the dominant polymer adsorption mechanism. Increasing the relative fraction of charged polymer molecules could increase the coverage of PEG on the microparticles, leading to a change in their interfacial activity or suppressing the contact line roughness.

In conclusion, we have investigated novel colloidal crystallization and polymer phase segregation occurring simultaneously and independently at the fluid–air interface in mixtures of aminated colloids and carboxylated PEG molecules. The particles exhibit interfacial activity, probably due to the adsorption of deprotonated polymer molecules on their surfaces. We employ the interfacial colloid dynamics to map the local microrheology and therefore the polymer concentration along the droplet's surface. Free polymer molecules spontaneously self-associate at the air–water interface, producing a 2-D network with a polymer-rich backbone and isolated, polymer-sparse islands. Sequential addition of particles to these areas generates structurally and dynamically distinct 2-D colloidal ensembles. Capillary interactions between mobile particles, induced by the combination of irregular contact lines and interfacial curvature, drive the formation of equilibrium 2-D crystals with square lattice geometry. Our current results unveil exciting new avenues of colloidal self-assembly with applications in photonics, lithography, and particle separations, and point to new directions for both computational and experimental studies of interfacial particle assembly using external curvature and intrinsic capillary quadrupoles. Additionally, the carboxylated PEG polymer can potentially serve as a stabilizing agent for foams and aerosols due to its unique interfacial activity and phase behaviour.

This work was supported in part by a UCI Graduate Dean's Dissertation Fellowship to MMS and the National Science Foundation (DMR-0706669). We gratefully acknowledge Bharath Rajaram for assistance with confocal microscopy, Matthew N. Lee for discussions related to image rendering, and an anonymous reviewer for suggesting the possible role of droplet curvature in quadrupolar interparticle interactions.

Notes and references

1 B. P. Binks, *Curr. Opin. Colloid Interface Sci.*, 2002, **7**, 21.
2 Z. Du, M. P. Bilbao-Montoya, B. P. Binks, E. Dickinson, R. Ettelaie and B. S. Murray, *Langmuir*, 2003, **19**, 3106.
3 R. Aveyard, B. P. Binks and J. H. Clint, *Adv. Colloid Interface Sci.*, 2003, **100–102**, 503.
4 B. P. Binks and T. S. Horozov, *Angew. Chem.*, 2005, **117**, 3788.
5 E. M. Herzig, K. A. White, A. B. Schofield, W. C. K. Poon and P. S. Clegg, *Nat. Mater.*, 2007, **6**, 966.
6 D. Lee and D. A. Weitz, *Adv. Mater.*, 2008, **20**, 3498.
7 F. Rossier-Miranda, C. Schroën and R. Boom, *Colloids Surf., A*, 2009, **343**, 43.
8 M. N. Lee and A. Mohraz, *Adv. Mater.*, 2010, **22**, 4836.
9 S.-H. Kim, S. Y. Lee, S.-M. Yang and G.-R. Yi, *NPG Asia Mater.*, 2011, **3**, 25.
10 J. Zhang, Y. Li, X. Zhang and B. Yang, *Adv. Mater.*, 2010, **22**, 4249.
11 P. Pieranski, *Phys. Rev. Lett.*, 1980, **45**, 569.
12 K. P. Velikov, F. Durst and O. D. Velev, *Langmuir*, 1998, **14**, 1148.
13 E. R. Dufresne and D. G. Grier, *Rev. Sci. Instrum.*, 1998, **69**, 1974.
14 K.-H. Lin, J. C. Crocker, V. Prasad, A. Schofield, D. A. Weitz, T. C. Lubensky and A. G. Yodh, *Phys. Rev. Lett.*, 2000, **85**, 1770.
15 J. Hur and Y.-Y. Won, *Soft Matter*, 2008, **4**, 1261.
16 S. O. Lumsdon, E. W. Kaler and O. D. Velev, *Langmuir*, 2004, **20**, 2108.

17 J. C. Crocker and D. G. Grier, *J. Colloid Interface Sci.*, 1996, **179**, 298.
18 A. D. Dinsmore, E. R. Weeks, V. Prasad, A. C. Levitt and D. A. Weitz, *Appl. Opt.*, 2001, **40**, 4152.
19 P. Ramachandran and G. Varoquaux, *IEEE Comput. Sci. Eng.*, 2011, **13**, 40.
20 T. Savin and P. S. Doyle, *Biophys. J.*, 2005, **88**, 623.
21 T. G. Mason, K. Ganesan, J. H. van Zanten, D. Wirtz and S. C. Kuo, *Phys. Rev. Lett.*, 1997, **79**, 3282.
22 J. A. Henderson, R. W. Richards, J. Penfold, R. K. Thomas and J. R. Lu, *Macromolecules*, 1993, **26**, 4591.
23 M. Winterhalter, H. Bürner, S. Marzinka, R. Benz and J. Kasianowicz, *Biophys. J.*, 1995, **69**, 1372.
24 J. Wu and L. L. Dai, *Langmuir*, 2007, **23**, 4324.
25 M. Oettel and S. Dietrich, *Langmuir*, 2008, **24**, 1425.
26 E. P. Lewandowski, J. A. Bernate, P. C. Searson and K. J. Stebe, *Langmuir*, 2008, **24**, 9302.
27 M. Cavallaro, L. Botto, E. P. Lewandowski, M. Wang and K. J. Stebe, *Proc. Natl. Acad. Sci. U. S. A.*, 2011, **108**, 20923.
28 A. Würger, *Phys. Rev. E: Stat., Nonlinear, Soft Matter Phys.*, 2006, **74**, 041402.
29 D. Stamou, C. Duschl and D. Johannsmann, *Phys. Rev. E: Stat. Phys., Plasmas, Fluids, Relat. Interdiscip. Top.*, 2000, **62**, 5263.
30 B. J. Park and E. M. Furst, *Soft Matter*, 2011, **7**, 7676.
31 P. A. Kralchevsky and N. D. Denkov, *Curr. Opin. Colloid Interface Sci.*, 2001, **6**, 383.
32 B. J. Park, T. Brugarolas and D. Lee, *Soft Matter*, 2011, **7**, 6413.

Addition and correction

Note from RSC Publishing

This article was originally published with incorrect page numbers. This is the corrected, final version.

The Royal Society of Chemistry apologises for these errors and any consequent inconvenience to authors and readers.